

ANALYSIS OF LIMB BRIGHTENING ON THE QUIET SUN AT 21 CM USING A THREE-ELEMENT INTERFEROMETER

Jonathon Oiler
Alan E.E. Rogers
MIT Haystack Observatory

ABSTRACT

During the summer, three small radio telescopes (SRTs) were used for observing the Sun during the Sun's Quiet Phase almost daily over a two month period. We used the three SRTs as a 3-element interferometer to observe the entire Sun. The baselines used were 7.77 meters, 20.12 meters, and 26.67 meters. Data from the Sun were taken and software was used to calculate the visibility amplitudes and closure phase. A modeling program was used to replicate the Sun and a comparison of closure phases between the SRT data and the modeling data was performed with a weighted least-squares fit. We found evidence for limb brightening around the equatorial region of the Sun and determined that the modeling software fit the data better with limb brightening (the outer 20 percent of the solar disk's diameter) used in conjunction with a translatable sunspot of varying brightness. The equatorial limb brightening was found to contribute 30 ± 10 percent of the total solar radio flux.

1.0 INTRODUCTION

This summer we used the three SRTs in a short-baseline interferometry pattern to observe the entire Sun. The main goal of watching the Sun was to verify and possibly improve upon limb brightening understanding as discussed in papers only as recent as 1970.

The presence of limb brightening on the Sun was first suggested by Martyn (1946). Rays traveling from the limb of the sun to the Earth have a longer path length through the corona as compared to rays traveling from the central meridian. This increased path length leads to an increase in optical thickness. The increased optical thickness causes the brightness temperature to increase at the limb (Smerd, 1950). The presence of limb brightening was later found to be in the equatorial region (constrained to ± 60 deg from the equator) and not in the polar region (Christiansen & Warburton, 1955). Roosen and Goh (1966) determined that not only was the brightening in the equatorial region but that it was offset on one side with respect the central meridian. Viewed at

21 cm, they determined that the offset was approximately 30° inside of the limb on the western side. A few years later, Simon and Zirin (1969) argued that new data showed there is no limb brightening anywhere between 3 \AA and 75 cm except at 1032 \AA (0.1 \mu m) and at 1.2 mm. They posited that the older instruments used in the previous observations had too low a resolution which led to a spurious brightening increase near the equatorial limb due to active regions on Sun. In later papers, argument had once again been made for the possible presence of limb brightening at shorter wavelengths, although none had looked the 21 cm wavelength.

2.0 SMALL RADIO TELESCOPES

The three SRTs (labeled SRT1, SRT2, and SRT3) used in the analysis each had a 2.3 m diameter. They were set up as a 3-element interferometer in a small triangle (Figure 1). The baselines of the interferometer were 7.77 m between SRT1 and SRT2, 20.12 m between SRT1 and SRT3, and 26.67 m between SRT2 and SRT3. The data sampling process is

controlled by the global positioning system (GPS). This allows the system to observe in a very long baseline interferometry (VLBI) mode where the SRTs track the sun for approximately 8 hours of the day.



Figure 1: The SRTs used in the 3-element interferometer. In the foreground is SRT3. The left-most antenna on the red trailer is SRT1 and the remaining antenna is SRT2.

For more information on the interferometer geometry calculations, see SRT Memo #018 in the appendix. The system records the data to a disk every 10 minutes at 10 second intervals. The data is transferred to a computer where it is correlated. From there, the baseline phases and normalized correlation are calculated. The phases are then used to calculate the closure phase.

3.0 CLOSURE PHASE

The closure phase is a method developed by Jennison (1958) for obtaining the amplitude and phase of a complex Fourier transform of a spatial brightness distribution. The method is used to self-calibrate the phase information. When the interferometer collects data, phase errors are introduced by a means of the electronic equipment, atmospheric effects and the geometry of the terrain that the interferometer is set-up in. If we let ϕ be the measured phase from the antennas, ψ be the phase of the transform, θ be the phase errors mentioned above and ϵ be the noise, then

$$\phi_{12} = \psi_{12} + \theta_1 - \theta_2 + \epsilon_{12}$$

$$\phi_{23} = \psi_{23} + \theta_2 - \theta_3 + \epsilon_{23}$$

$$\phi_{31} = \psi_{31} + \theta_3 - \theta_1 + \epsilon_{31}$$

where the subscripts represent the phase on the baseline between the different telescopes. When these equations are added together, the sum

$$\phi_{12} + \phi_{23} + \phi_{31} = \psi_{12} + \psi_{23} + \psi_{31} + \epsilon_{12} + \epsilon_{23} + \epsilon_{31},$$

where $\phi_{12} + \phi_{23} + \phi_{31} = \phi_{123}$, is called the closure phase. By adding the three equations together, the phase errors were eliminated. Knowing the noise of each system allows the determination of the phase of the Fourier transform. The method for calculating the amplitude can be found in Jennison (1958). The source structure can then be modeled to fit the closure phase and amplitudes on the 3 baselines if simple structures which can be characterized by a few parameters are considered. The modeling software and the parameters used with it will be discussed in the next section.

4.0 SOFTWARE

Before the modeling software is detailed, a description of the GUI interface between the user and the telescopes will be discussed. The GUI program allows the user to choose a source for tracking by each or all of the SRTs. This program also has capabilities in “VLBI mode” to continuously track the source and make recordings at specific intervals of the GPS timer. The program also allows for users to check for pointing errors and correct for them through the command “npoint”. The n-point check creates an image for the user with the pointing error offset printed below (Figure 2). For this analysis, these were the main features that were used. A screenshot of the GUI can be found in the appendix.

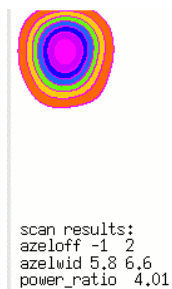


Figure 2: The results of a pointing error scan.

The main data analysis program was called “sunspot.” The program’s aim was to model the Sun as a uniform disk with an unresolved sunspot of varying flux, position angle, and radial distance from the center of the disk. The model produces a closure phase and amplitude which can be compared the actual observed closure phase and amplitude. The program searches through the parameter space to find the best fit between the two closure phase plots (actual data vs. model data) over the day by minimizing the sum of the residuals squared (least-squares) for N observations on each day (Figure 3).

$$\sum_j \sum_i (m_{ij} - a_{ij})^2 + \sum_j (\cos(mc_j) - \cos(c_j))^2 + \sum_j (\sin(mc_j) - \sin(c_j))^2$$

m_{ij} = model amplitudes
 a_{ij} = observed amplitudes
 mc_j = model closure phases
 c_j = observed closure phases
 i = baseline index, 0 to 2
 j = time index, 0 to N-1

Figure 3: Mathematical equation representing the weighted least squares minimization.

The program output called “srt.pos” prints a picture of best fit model with sunspot included (Figure 4). The model’s picture of the sun for all days analyzed can be found in the appendix. A comparison plot of the sun as viewed from the SOHO satellite on the same day the data was taken is provided as a reference and comparison (Figure 5). The program also plots the best fit closure phase plot determined by the least squares method and outputs the plot along with

the plot of the actual closure phase from SRT data. An image of that plot can be found in the appendix.

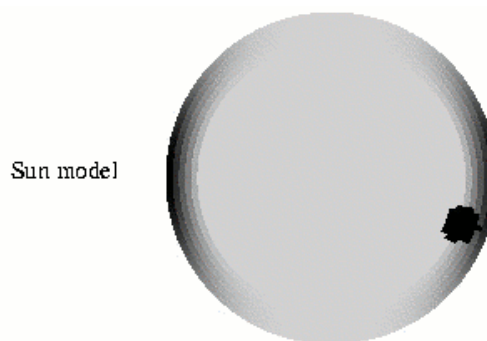


Figure 4: The printed model of the Sun as determined by the least squares fit on July 7, 2006. The darker colors along the edges represent the limb brightening and will be discussed in detail later. The black circular shape represents a sunspot at a location predicted by the model.



Figure 5: The Sun as pictured by the SOHO satellite on July 7, 2006. The location of the sunspot matches closely to that predicted with the model program.

5.0 RESULTS AND DISCUSSION

The SRT interferometer data was taken between June 6, 2006 and July 29, 2006 while the Sun was relatively quiet (Figure 6). Sunspots can influence the data because they are regions of increased solar radio flux and in order to determine whether there was an increase of flux

from the limbs, minimal sunspot influence on the data was desired.

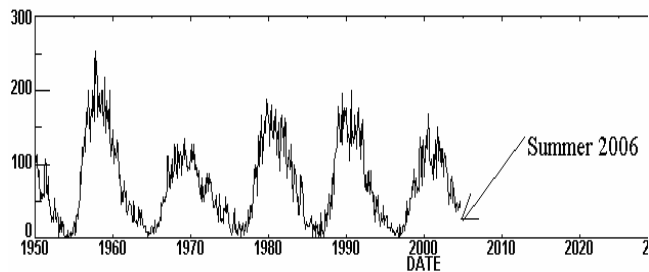


Figure 6: A plot of the monthly average number of sunspots versus time of the year. As pointed out, data was taken near the sunspot minimum (solar minimum) which allowed for minimal influence on the data from active regions.

The sunspot program outputs the closure phase best fit value as well as brightness amplitude and those numbers were recorded in Microsoft Excel. The main sunspot program was slightly altered in order to adjust the location of the limb brightening to check for polar brightening and look for any offset brightening as was described in Roosen and Goh (1966).

5.1 LIMB BRIGHTENING

The model was firstly setup to make a comparison between SRT data and a uniform circular disk with an optical radius. The data was not found to be a good fit. Next, circularly symmetric limb brightening was added at a distance beyond 80 percent of the solar radius (Figure 7).

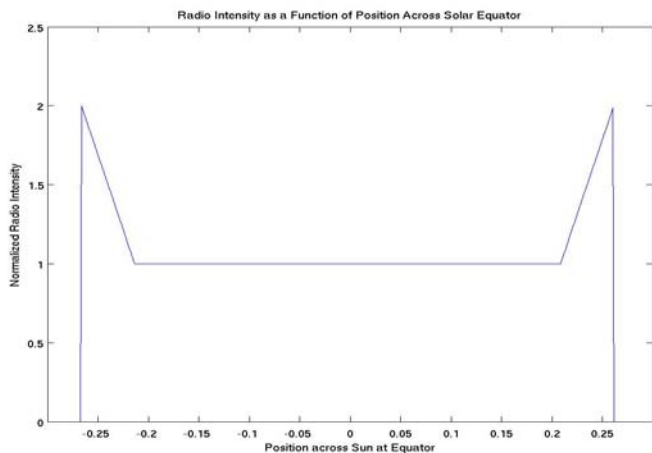


Figure 7: A graphical depiction of how the brightening was added.

The data was not found to be a good fit as well. Thirdly, the limb brightening was constricted to the equatorial region by multiplying the circularly symmetric limb brightening equation by a factor of \cos^2 of the angle swept out around the circular disk starting at the equator. The data was found to be a good fit (Figure 8). The plot takes the best fit value from various strengths of limb brightening. In all plots the best fit value is defined as the root mean square of the residuals in fractional units. Thus a best fit value of 0.05 corresponds to an average error of five percent in visibility and five percent of a radian or 3 degrees in closure phase. The strength of limb brightening was plotted as a ratio of strength of brightening in the limb compared to the strength in the rest of the disk. The ratio ranged from 0 to 10. A plot of the best fit limb brightening ratio over all days is provided in Figure 9. This plot has one large peak. The peak coincides with a time when a very large sunspot was present. Therefore this value may not represent the actual limb brightening due to possible sunspot influence.

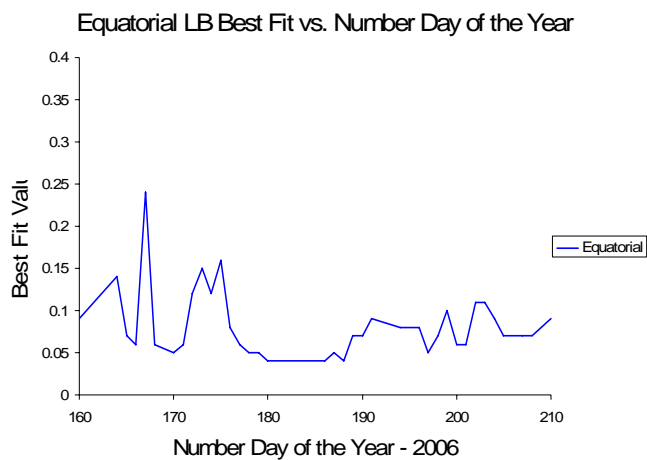


Figure 8: A plot of the best fit value of equatorial limb brightening over all days. Various amounts of limb brightening were considered for each day of data and the amount that provided the best fit was used in this plot.

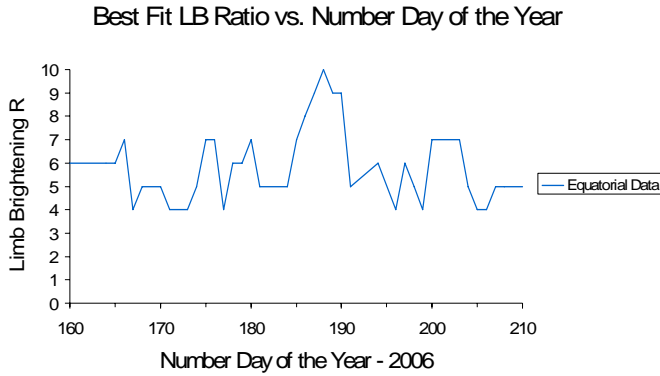


Figure 9: A plot of the best fit limb brightening ratio (ratio of the strength of brightness in the limb to the brightness in the rest of the disk). The two peaks at a ratio of 10 correspond to high sunspot frequency and may have influenced the determination the limb brightening ratio.

The mean strength of the limb brightening ratio was found to be approximately five (Figure 10). However, this value is somewhat arbitrary based on how spread out or concentrated one makes the area over which there is limb brightening. Therefore, a better representation of the amount of limb brightening is the ratio of the total flux in the limb versus the total flux in the whole disk (limb included). This value was determined to be approximately 0.3 ± 0.1 . From a diagram in Christiansen and Warburton (1955), an estimation of the total flux ratio that they found was about 0.1. We have found more contribution to the total flux from the limb.

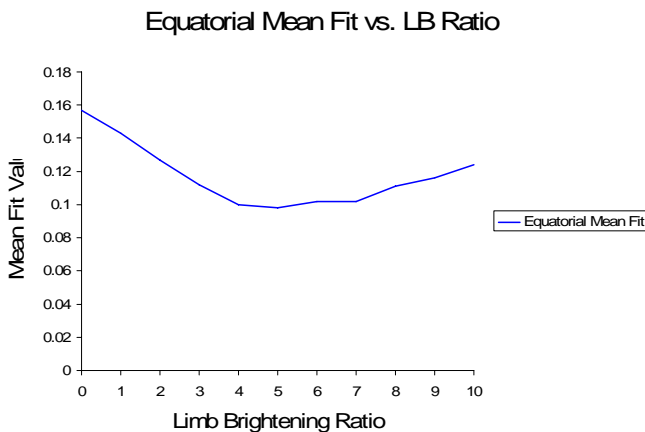


Figure 10: Mean Fit Value of each limb brightening ratio over all days. The curve hits a minimum somewhere around 5 although is very shallow between the values of 4 and 6.

To verify the legitimacy of the equatorial limb brightening, a comparison to limb brightening in the polar region only was made. Basically the equatorial limb brightening was rotated 90 degree and the same analysis done. A comparison of the best fit value over all the days between the equatorial data and the polar data found that the equatorial data was a much better fit (Figure 11). There is a region of graph where the fit was extremely good (between day 180 and 189) and during this range of days a very large sunspot was present. The limb brightening best fit value for the polar data was a ratio of 0 (no limb brightening) for every day of the data. The polar limb brightening fit increased as the ratio was increased (Figure 12), showing strong proof for equatorial limb brightening.

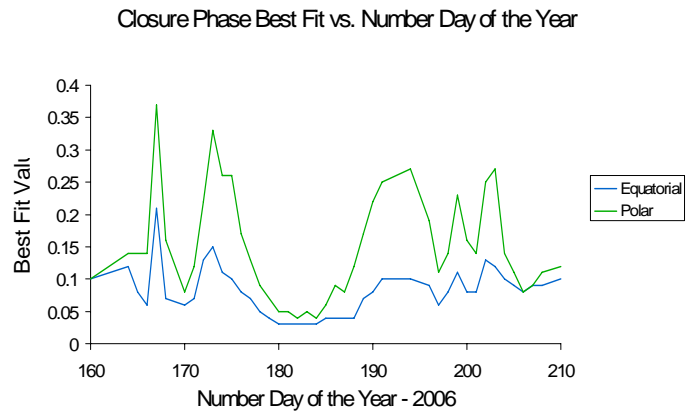


Figure 11: A plot of the best fit value of equatorial data (blue) and the best fit value of the polar data (green) over all days. Every best fit value from the polar data came from a limb brightening ratio of 0 (no limb brightening).

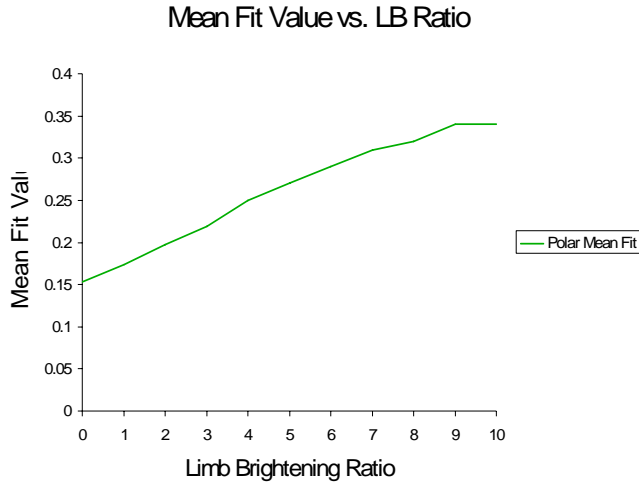


Figure 12: A plot of the mean best fit value over all values of the limb brightening ratio. The graph shows that adding any limb brightening at all causes the fit to become less accurate. The graph represents what happened for every day of data analyzed.

Based on data recently collected from the Ulysses spacecraft (McComas et. al, 2000) an explanation for the brightening found only in equatorial region can be given. The strong magnetic fields emanating from the Sun's poles have caused a concentration of electrons in the equatorial region (Figure 13).

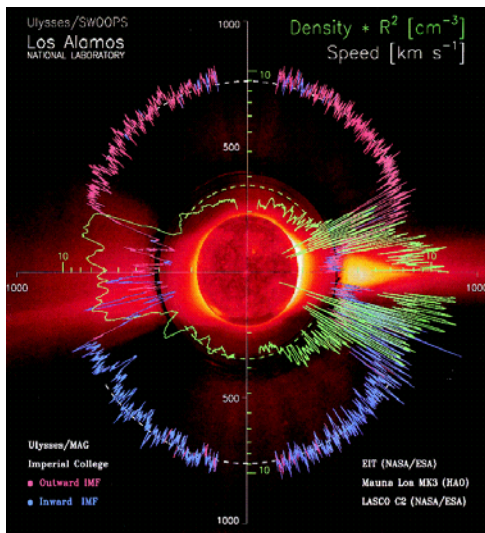


Figure 13: An image of the Sun with electron density plotted (green line). The plot shows the density to be highly concentrated around the equatorial region, which provides an explanation for the equatorial brightening.

The reason for this is because near the Sun, the magnetic field strength dominates the electrons' kinetic energy and therefore the electrons are constrained to move only along the magnetic field lines. At the poles, the magnetic field lines are mostly open, allowing the electrons to escape into space. Near the equator, the field lines are mostly closed, confining the electrons to the equatorial region. The increase of electrons around the equator results in an increase in optical depth in that area and therefore the brightness temperature increases.

5.2 OFFSET BRIGHTENING

The paper from Roosen and Goh (1966) described the limb brightening as being offset on one side. After looking at where the limb brightening was, we wanted to see if we could determine whether or not the brightening was offset on one side. To accomplish this, the sunspot modeling software was edited to have the brightening fixed on one limb and allow the limb brightening on the other side of the disk to essentially move across half of the disk. The strength of the brightening was also a variable that left to be determined by the simulation. Because of the complexity of the calculation and run-time considerations, the roaming sunspot was removed from the program. A comparison of equatorial brightening with no offset to equatorial brightening with a variable offset showed that the equatorial brightening with no offset was a better fit (Figure 14). However, we do not think that this shows that the offset brightening is an incorrect model because we could not directly compare the two as the best equatorial data with limb brightening involved using a sunspot but the offset brightening did not have a sunspot.

perform research in the area of Astronomy/Astrophysics and I gained a lot of respect for the power of radio astronomy.

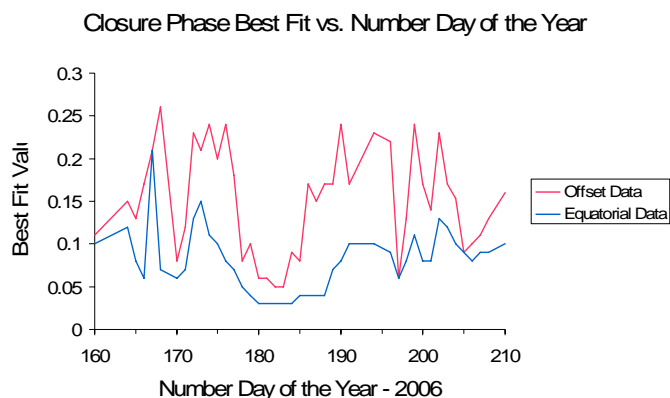


Figure 14: A comparison plot of the best fit value over all days between the equatorial limb data (blue) and the equatorial offset data (red). Because the offset program could not incorporate a sunspot, this is not a direct comparison and does not prove that the limb brightening is not offset.

In future analyses, a way to compare the two programs would be to set the limb brightening at the offset of $\sim 30^\circ$ as described in Goosen and Roh (1966). Then if the sunspot is added to the offset program and brightening is varied the same a better comparison can be made. Also, if the position of the best fit sunspot can be determined using the equatorial limb data, then the offset program could analyze each day with the same sunspot position and then allow the offset to vary, a best position of the offset could be determined over all days.

6.0 CONCLUSION

This summer we used the SRTs in a three-element interferometer to look at limb brightening of the Sun. We found that there is limb brightening in the equatorial region of the sun with an approximate total solar flux in the limb compared to the overall disk of 0.3 ± 0.1 .

On a personal note, I gained a lot of experience using various software programs for using the SRTs and modeling the data. I learned a lot about the Sun and gained a lot of experience programming in C and Python. I enjoyed collaborating with others and appreciated the amount of support and independence that I was given in my project. This program has really affirmed my desire to go to graduate school and

X. REFERENCES

Christiansen, W.N. and Warburton, J.A., 1955 Aust.

Jennison, R.C., 1958, RAS

Martyn, D.F., 1946, Nature, 158, 632

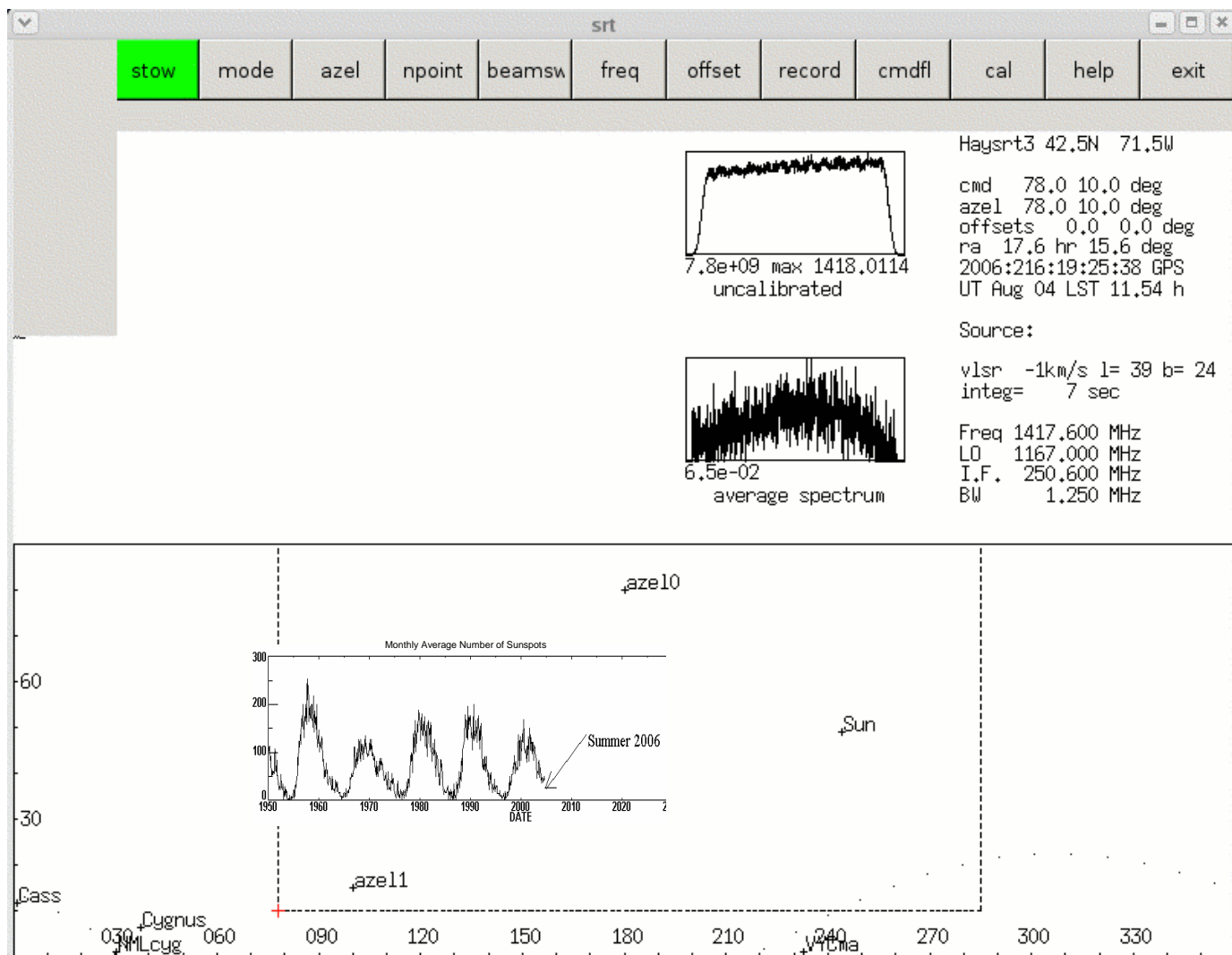
McComas et al., 2000, JGR, 105, A5, 10,419

Roosen, J. and Goh, T., 1967, Solar Physics

Simon, M. and Zirin, H., 1969, Solar Physics, 9, 317

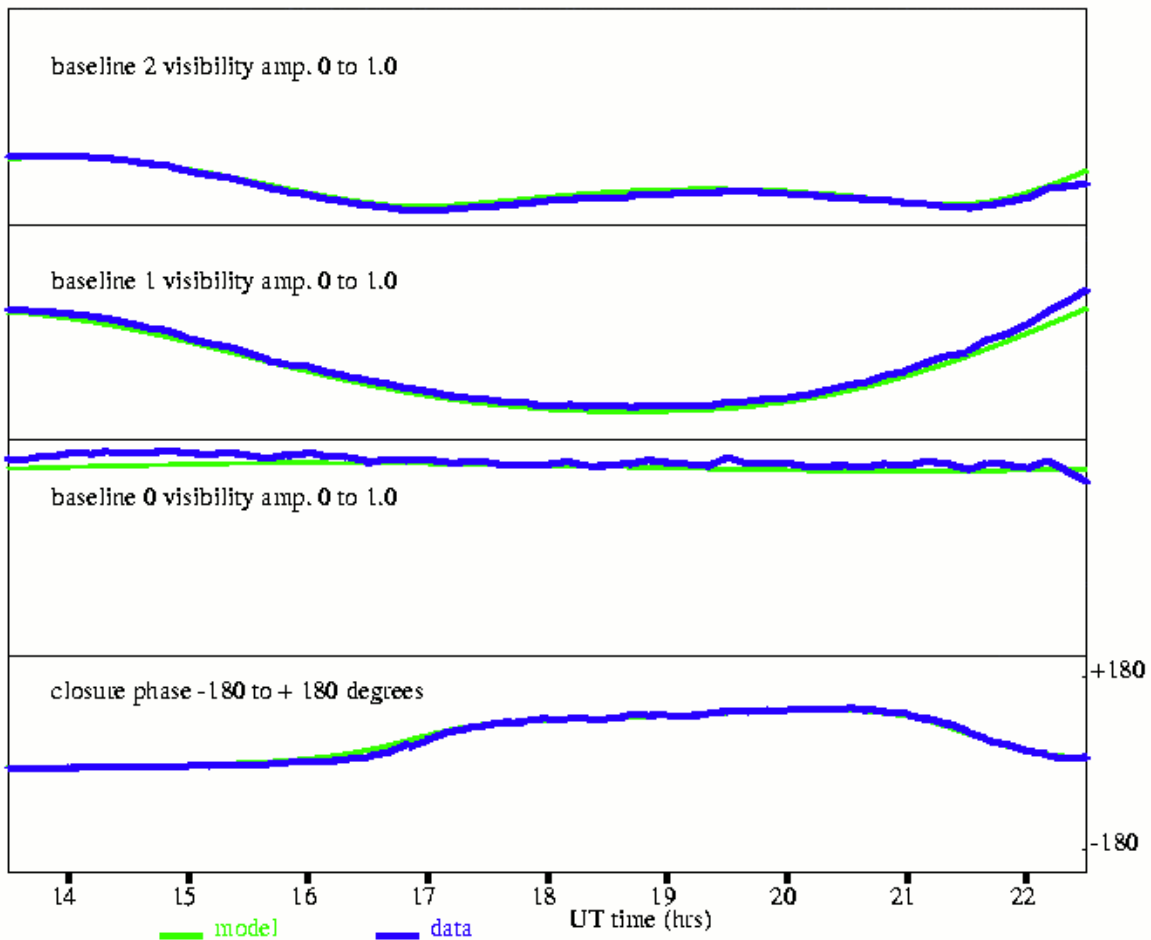
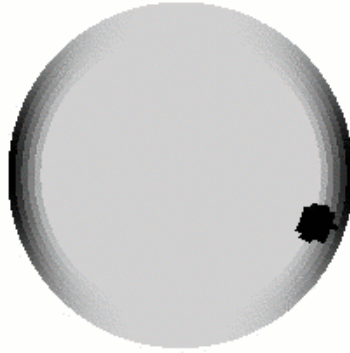
Smerd, S.F., 1950, Aust. J. Sci. Res., A3, 34

X. APPENDIX



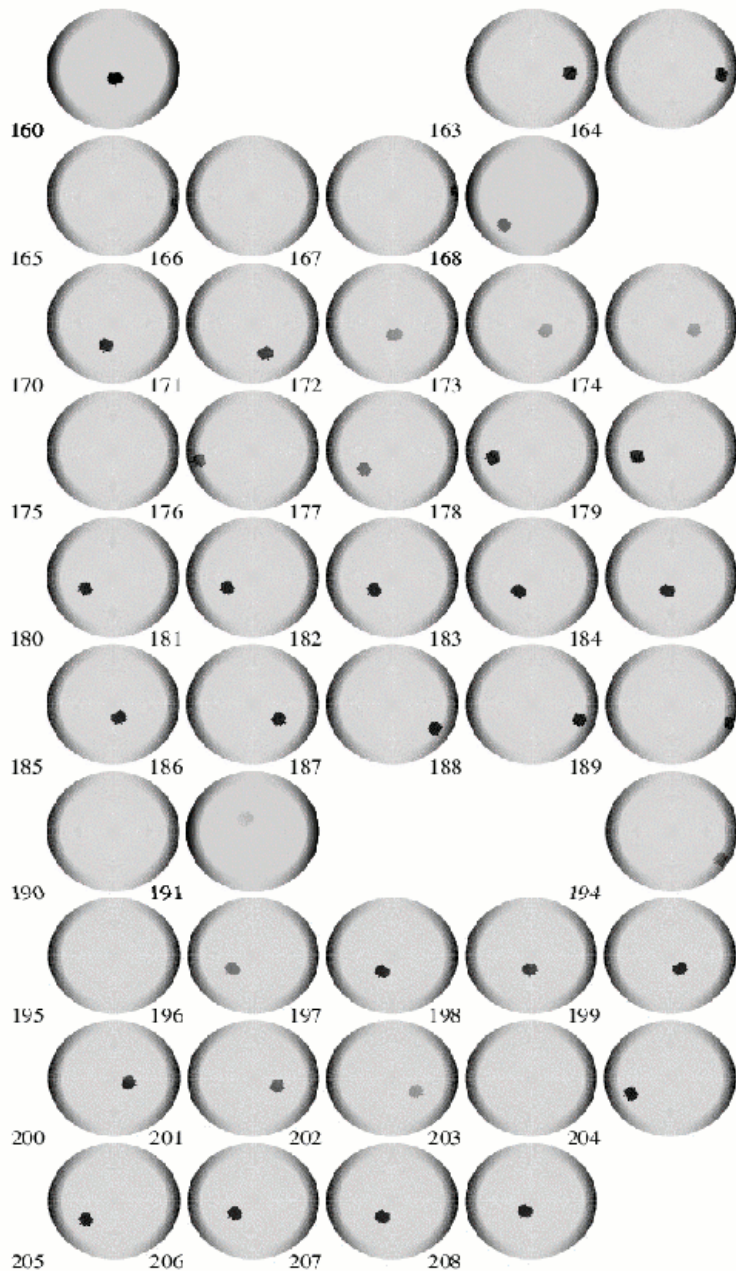
GUI program for using one of the SRTs.

Sun model



fit 0.04 baam 0.10 limb brightness ratio 5.00 limbfrac 0.26
/data1/srt/2006_188_13_30.Haysrt2 /data1/srt/2006_188_13_30.Haysrt3
/data1/ent/2006_188_22_30.Haysrt2 /data1/ent/2006_188_22_30.Haysrt3

Output of the sun modeling program on July 7, 2006. The lower plot is a plot of the closure phase from the SRT data (blue line) and the corresponding model closure phase plot (green line). The least squares fit is calculated using these two lines and is 0.04 on this day, which is an excellent fit.



Sunspot program's output of the best fit images over most days in the range of the study.